Mechanical picture of the linear transient growth of vortical perturbations in incompressible smooth shear flows

George Chagelishvili,[1,2] Jan-Niklas Hau,[3,4,*] George Khujadze,[5] and Martin Oberlack[3,4]
[1]*Abastumani Astrophysical Observatory, Ilia State University, Tbilisi 0160, Georgia*
[2]*M. Nodia Institute of Geophysics, Tbilisi State University, Tbilisi 0128, Georgia*
[3]*Chair of Fluid Dynamics, Department of Mechanical Engineering, Technische Universität Darmstadt, Otto-Berndt-Strasse 2, 64287, Darmstadt, Germany*
[4]*GSC CE, Technische Universität Darmstadt, Dolivostraße 15, 64293 Darmstadt, Germany*
[5]*Chair of Fluid Mechanics, Universität Siegen, Paul-Bonatz-Str. 9-11, 57068 Siegen, Germany*
(Received 25 January 2016; published 4 August 2016)

The linear dynamics of perturbations in smooth shear flows covers the transient exchange of energies between (1) the perturbations and the basic flow and (2) different perturbations modes. Canonically, the linear exchange of energies between the perturbations and the basic flow can be described in terms of the Orr and the lift-up mechanisms, correspondingly for two-dimensional (2D) and three-dimensional (3D) perturbations. In this paper the mechanical basis of the linear transient dynamics is introduced and analyzed for incompressible plane constant shear flows, where we consider the dynamics of virtual fluid particles in the framework of plane perturbations (i.e., perturbations with plane surfaces of constant phase) for the 2D and 3D case. It is shown that (1) the formation of a pressure perturbation field is the result of countermoving neighboring sets of incompressible fluid particles in the flow, (2) the keystone of the energy exchange mechanism between the basic flow and perturbations is the collision of fluid particles with the planes of constant pressure in accordance with the classical theory of elastic collision of particles with a rigid wall, making the pressure field the key player in this process, (3) the interplay of the collision process and the shear flow kinematics describes the transient growth of plane perturbations and captures the physics of the growth, and (4) the proposed mechanical picture allows us to reconstruct the linearized Euler equations in spectral space with a time-dependent shearwise wave number, the linearized Euler equations for Kelvin modes. This confirms the rigor of the presented analysis, which, moreover, yields a natural generalization of the proposed mechanical picture of the transient growth to the well-established linear phenomenon of vortex–wave-mode coupling.

DOI: 10.1103/PhysRevFluids.1.043603

I. INTRODUCTION

Flows with nonuniform mean velocity profiles are ubiquitous in both nature and the laboratory, occurring in broad areas such as atmospheres and oceans, stars and astrophysical accretion disks, as well as tokamak reactors and other technical flow systems. Beyond any doubt, dynamical phenomena associated with nonuniform kinematics and inhomogeneity of thermodynamic quantities are of equal importance.

In the 1990s it was finally revealed and mathematically rigorously proven that the classical modal analysis, spectral expansion of perturbations in time, is far from being optimal to study the linear perturbation dynamics in smooth shear flows. Moreover, it sometimes leads to fundamental problems. The reason is found in the mathematical specificity of such flow systems when applying the modal analysis, as the appearing operators are nonnormal (nonself-adjoint), and, consequently, the corresponding eigenmodes are nonorthogonal [1–5]. Evidently, the nonorthogonality leads to

*hau@fdy.tu-darmstadt.de

strong interference among the eigenmodes, and, thus, a proper or, one can say, optimal approach should be capable of fully analyzing this. While possible in principle, this is a formidable task in practice. In fact, the result obtained from the analysis of separate eigenfunctions and eigenvalues is far from complete. So, for a correct and full description of the shear flow phenomena, one needs to know the interference processes, which, yet, cannot be easily taken into account in the framework of the modal analysis. Here the focus lies on the asymptotic stability of flows, and little attention is paid to any particular initial value or finite time period of the dynamics. Indeed, the transient evolution is regarded as having no significance and left for speculation. Around the 1990s, the emphasis was shifted from the analysis of the long-time asymptotic flow stability to the transient behavior. Analyzing the latter by employing the so-called nonmodal approach, the linear transient growth of perturbations in asymptotically or spectrally stable hydrodynamic shear flows was demonstrated [1,6].

The nonmodal analysis is a modification of the initial value problem and is capable of revealing several unexpected phenomena, which were overlooked by the modal analysis. There exist two different formulations of the nonmodal approach: the generalized stability theory [7] and the Kelvin mode approach. These approaches have enjoyed substantial success in furthering an adequate description of instabilities and in providing the missing linear and nonlinear dynamics in a variety of shear flows. We base our investigation on the celebrated Kelvin mode approach (stemming from the 1887 paper by Lord Kelvin [8]) that became well established and extensively used since the 1990s. It is the simplest formulation and involves the change of the independent variables from the laboratory to a moving frame and allows us to quantitatively study the temporal evolution (the short-term behavior) of spatial Fourier harmonics (SFHs) of perturbations without any spectral expansion in time. *De facto*, these modes represent the "simplest element" of shear flow dynamics [9]. This approach not only describes systems with constant shear flow, but also guides the understanding and qualitative description of smooth shear flow phenomena. We note here that there exists various terminology for the Fourier mode with time-dependent wave vector in the different communities, e.g., "Kelvin mode," "shear wave," "shwave," and "flowing eigenfunctions." Salhi and Cambon [10] give a comprehensive survey of the method in the different communities (see Secs. I and II C).

The central question that arises is to find the generic mechanical basis of the linear dynamics in these flows. We follow the widely accepted way of investigating fluid or plasma instabilities, namely, introducing fluid particles that undergo a small spatial shift in the flow and subsequently analyzing the resulting variance of the forces acting on the particles. This is illustrative to understand the problems of convective instability or internal gravity waves in vertically, i.e., parallel to the gravity force, stratified fluid dynamics [11], Parker instability in horizontally magnetized and vertically stratified fluids [12], and magneto-rotational instability in rotating magnetized flows [13]. Hence, its application to shear flows seems reasonable, especially as all forces are taken into account, including the pressure force. This force, in some sense "invisible" as it does not perform any work, is absent in the energy balances of the dynamics. So, at first glance, it seems preferable to analyze the dynamics with the help of the vorticity dynamics equations, which leave the pressure force out of sight. Having said that, the transient growth dynamics are mainly analyzed in terms of the Orr [14] and lift-up mechanisms [3,15]. These, however, do not provide any obvious link between each other, giving the impression that two different mechanisms are at work, one for the 2D and another for the 3D case. Chagelishvili *et al.* [9] have proposed to analyze the mechanistic picture that leads to the transient growth of perturbations, by shifting the focus towards the pressure force, i.e., the main factor of the dynamical activities. They have considered the dynamics of the plane perturbation that are imposed in a 2D plane flow with constant shear of velocity, $\mathbf{U} = (Ay,0)$, in terms of fluid particle dynamics. The role of the pressure was first theoretically investigated by Batchelor [16] in turbulent flows. Since then, it has been shown, both experimentally and numerically (e.g., see Refs. [17–22]), that the pressure forces provide the main mechanism to redistribute kinetic energy among fluid elements, without making a net contribution to the overall energy budget. However, the subject of the analysis was homogeneous and isotropic turbulence. Yet the isotropy is the limiting factor in the applicability of the formed concepts to nonuniform (anisotropic) flows. In fact, the appearance of pressure forces in

the Navier-Stokes equation is due to linear and nonlinear processes; specifically, it is caused by linear and nonlinear combinations of velocity perturbations. As follows from Ref. [23], in the isotropic case, the pressure terms are caused by nonlinear combinations of velocity perturbations, whereas, in the anisotropic case, also by linear ones. The linearly and nonlinearly originated pressure terms feed back differently (independent from each other) on the velocity perturbations. According to Pumir *et al.* [22] the nonlinearly generated pressure terms show fundamentally different physics in 2D and 3D flows in the isotropic case. While the pressure forces strongly accelerate the fastest fluid elements in three dimensions, this effect is absent in two. This view, however, does not cover shear flows that are anisotropic and where pressure terms that origin from linearity may be dominant, which issue is considered in the present study by exclusively considering linear, transient perturbation dynamics.

We primary introduce the mechanical basis of the transient dynamics, by considering the dynamical picture of the interplay of multiple fluid particles in order to grasp the appearance of the pressure perturbation. This is identified as the crucial and leading player in the flow dynamics. Subsequently, the linearized Euler equations are constructed by following the dynamics of a single fluid particle and its interaction with the formed "pressure wall," hereby capturing the cause of the growth and its transient nature. This logically confirms the validity and exactness of the proposed mechanical picture.

The aims of this paper can be summarized as follows: (1) to extend the framework introduced by Chagelishvili *et al.* [9] for 3D plane shear flows; (2) to demonstrate that the transient growth mechanism is generic and equally applicable to 2D and 3D cases, differing only quantitatively; in this framework it becomes possible to explain why 3D growth appears at later stages, when the sheared plane waves (i.e., Kelvin modes) are tilted with the background flow and why the growth of 3D Kelvin modes greatly exceeds the growth of 2D ones; and (3) to construct the linearized Euler equations on the basis of the proposed mechanical picture.

The outline of the paper is as follows: In Sec. II we provide a description of the mechanical picture of the transient growth in the 2D case and construct the dynamical equations on this basis, which is extended to the 3D case in Sec. III. The conclusion and discussion are given in Sec. IV. Finally, the linearized Euler equations for the Kelvin modes in inviscid plane constant shear flows are presented in the Appendix.

II. THE MECHANICAL PICTURE OF THE 2D TRANSIENT GROWTH

Adopting the idea of Chagelishvili *et al.* [9], we suggest a qualitative and quantitative analysis of the underlying mechanical picture of the transient growth and its consequences in the 2D case: how pressure perturbations appear in shear flows and how the pressure force ensures the transient growth of vortex mode perturbations. By taking the pressure force directly into account, we show that it is the keystone of the amplification of vortex mode perturbations in incompressible smooth shear flows.

A. A qualitative analysis

The entire analysis can be explained in terms of Kelvin waves, i.e., plane perturbations or single SFHs that are imposed in an unbounded inviscid base flow with constant shear of velocity, $\mathbf{U} = (Ay,0)$. We consider an initially imposed plane perturbation with velocity field $\mathbf{u} = (u_x,u_y)$ that is presented in Fig. 1. This perturbation velocity field has the following phases: $\psi_{u_x} = k_x x + k_y y + \pi/2$ and $\psi_{u_y} = k_x x + k_y y - \pi/2$. Here x and y correspondingly denote the stream- and shearwise directions, and $\mathbf{k} = (k_x,k_y)$ is the wave number vector that is perpendicular to $\mathbf{u} = (u_x,u_y)$, as in the incompressible limit $\mathbf{k} \cdot \mathbf{u} = 0$.

The presentation of the suggested mechanism proceeds in the description of three processes, where the latter is based on the former: (1) the interplay of two single, distinct (virtual) fluid particles with the background flow; (2) generalization on a large amount of such particles, interacting with each

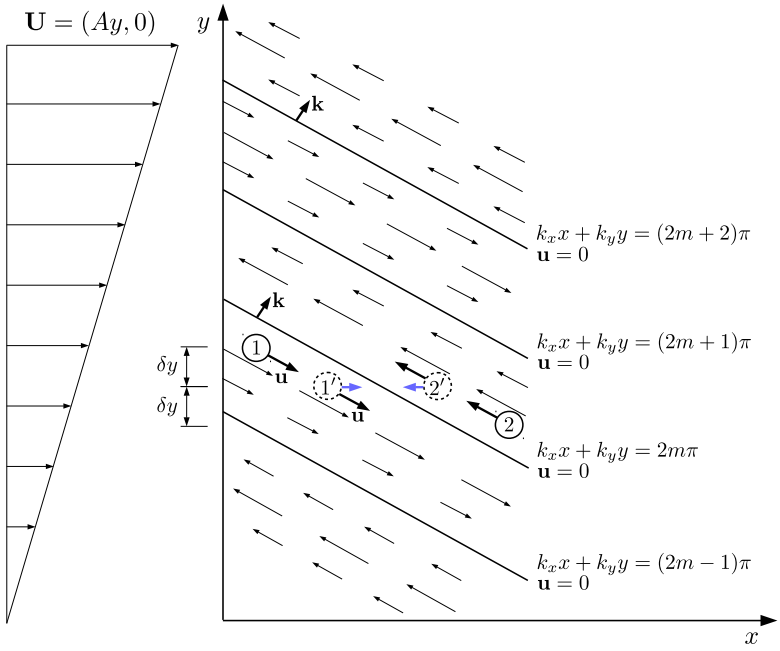

FIG. 1. A sketch illustrating the initially introduced velocity perturbation field, which is tilted opposite the shear. The solid lines indicate the lines of constant phase.

other and thereby inducing a pressure wall; and (3) finally, the description of the interaction of the multitude of fluid particles with the formed pressure perturbation wall.

Following this route, at first, we describe the induction of the pressure perturbation field due to the interplay of the background and perturbation velocity fields. In order to understand the cause of the appearance of the pressure perturbation, we consider two single virtual fluid elements (particles) at an arbitrary time, initially located on both sides of the zero-velocity perturbation lines, $k_x x + k_y y = 2\pi m$, in circles 1 and 2 (see Fig. 1). The fluid particles 1 and 2 are, respectively, located at levels y and $y - 2\delta y$, having oppositely directed perturbation velocities.

The unperturbed velocity of the fluid particle 1 is determined by the background velocity $\mathbf{U} = (Ay,0)$. Due to its shearwise perturbation velocity, u_y, this fluid particle is shifted downwards from its initial level y by δy to its new location (circle 1′) during a short period of time (δt). At its new level, the fluid particle "feels" a reduced unperturbed velocity of the background flow, i.e., $U - |\delta U| = A(y - \delta y)$. Thus, the velocity of the considered fluid particle can be rewritten as

$$\mathbf{U}(y) + \mathbf{u} = (Ay,0) + \mathbf{u} = (A(y - \delta y),0) + (A\delta y,0) + \mathbf{u}.$$

It follows that the fluid particle moves by δU faster in streamwise direction at its new location than the background flow:

$$\mathbf{U}(y) + \mathbf{u} = \mathbf{U}(y - \delta y) + \delta\mathbf{U} + \mathbf{u}. \tag{1}$$

The additional (relative to the basic flow) streamwise velocity of the fluid particle 1′, $\delta\mathbf{U}$, is presented by the blue arrow in Fig. 1. Analogously, the second fluid particle, circle 2, is shifted upwards by δy from its level $y - 2\delta y$ during δt and moves to its new location (circle 2′). Here, the unperturbed velocity of the background flow is by $|\delta U| = A\delta y$ higher. So the fluid particle 2′ moves slower by $|\delta U|$ relative to the basic flow (see left directed blue arrow of particle 2′). Hence, the blue arrows in the figure show that, due to the described process, a countermotion of the fluid particles 1′ and 2′ is induced.

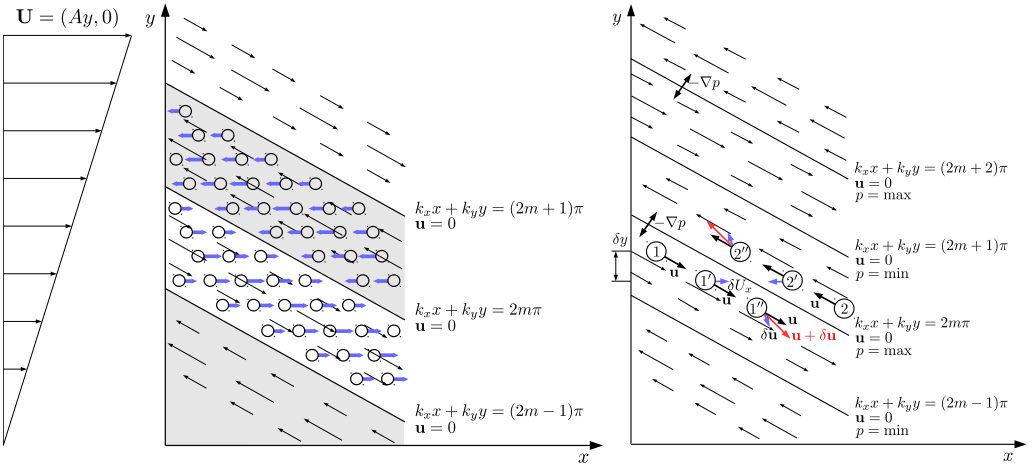

FIG. 2. Qualitative sketches illustrating (a) the induction of the pressure perturbation and (b) the mechanical picture of energy transfer from a shear flow to a single SFH, initially located at $k_y/k_x \gg 1$. (a) The dynamical interplay of a multitude of fluid particles from both sides of the zero perturbation velocity lines, $k_x x + k_y y = 2\pi m$, i.e., from both sides of the pressure wall ($p = \max$), is found to be the basis of the of the pressure induction. (b) The circles $1,1'$ and $1''$, or equally $2,2'$ and $2''$, indicate arbitrarily chosen virtual particles at different times. The lines $k_x x + k_y y = 2m\pi, (2m+2)\pi$ and $k_x x + k_y y = (2m+1)\pi$ respectively represent the intersections of the maximum and minimum pressure planes with the $z = 0$-plane.

To grasp the appearance of the pressure perturbation we generalize the above dynamical picture, considering the dynamical interplay of multiple fluid particles on both sides of the zero velocity perturbation lines, $k_x x + k_y y = 2\pi m$, as illustrated in Fig. 2(a). As described above, depending on the sign of u_y, fluid particles are shifted in opposite shearwise directions on different sides of the lines of $\mathbf{u} = 0$. Consequently, the additional streamwise velocities of these particles, δU, are oppositely directed (compare $\delta\mathbf{U}$ of the fluid particles coming from the white and gray zones). This countermotion leads to a compression of the medium, i.e., to a continuous rise of *the pressure perturbations*, with maximums ($p = \max$) at the lines of $k_x x + k_y y = 2\pi m$. Similarly, one can show that the minimums of the pressure perturbation coincide with the lines of $k_x x + k_y y = (2m + 1)\pi$, i.e., the extrema of the pressure perturbation field coincide with the lines of zero velocity perturbations, $\mathbf{u} = 0$. At the same time, the forces resulting from the pressure gradient (∇p) are parallel to the wave number vector (with $k_y/k_x > 0$ initially) and perpendicular to the maximum (minimum) pressure lines.

Further, in order to investigate the transient growth of vortical perturbations we analyze the dynamics of a single fluid particle in the pressure field. The induced pressure forces to turn each fluid particle around: a particle from one side of the maximum pressure line (i.e., a particle from the white side) in one direction and from the other side (i.e., a particle from the gray side) in the opposite direction. Therefore, one can consider the pressure perturbation field as an extended "pressure wall," from which the fluid particles are continuously reflected, obeying the laws of the elastic collision theory. Each of these walls is a mediator in the process of momentum exchange between a multitude of fluid particles from the white and gray zones shown in Fig. 2(a).

It follows from Eq. (1) that the single fluid particle will impinge on the "pressure wall" with the "collision velocity" $\delta\mathbf{U}$. In accordance with the theory of elastic collision of particles with a rigid wall, the incoming angle and velocity value of the respective particle equal the outgoing ones. As a result, the collision velocity $\delta\mathbf{U} = (\delta U, 0)$ is transformed to $\delta\mathbf{u} = (\delta u_x, \delta u_y)$, and thus, the postcollision perturbation velocity is changed to $\mathbf{u} + \delta\mathbf{u}$ [with $|\delta\mathbf{u}| = |\delta\mathbf{U}|$; see Fig. 2(b)]. For the

particular stage of the mechanistic picture (with $k_y/k_x > 0$) that is considered in this figure the angle θ between $\mathbf{u}$ and $\delta\mathbf{u}$ is less than $\pi/2$, i.e., $\theta < \pi/2$. This results in $|\mathbf{u} + \delta\mathbf{u}| > |\mathbf{u}|$, which is depicted by the red vectors at point $1''$ in Fig. 2(b); the energy of the single separated particle increases at the expense of the mean flow. The described energy growth connected to a single fluid particle [e.g., particle 1 in Fig. 2(b)] can be understood as the sequence of two processes:

(1) A shift of the fluid particle (due to the shearwise perturbation velocity u_y) from its original level y by δy to its new location during a short period of time, δt. The velocity of the fluid particle is constant during the shifting, and hence, it will move faster in its new location compared to the background flow.

(2) Due to this additional streamwise velocity, $\delta\mathbf{U}$, the particle collides elastically with the "pressure wall," and this collision velocity ($\delta\mathbf{U}$) is transformed into the additional perturbation velocity $\delta\mathbf{u}$, with $|\delta\mathbf{u}| = |\delta\mathbf{U}|$. After the collision the perturbation velocity has changed to $\mathbf{u} + \delta\mathbf{u}$; the elastic collision changes the value as well as the orientation of the perturbation velocity. While the change in $|\mathbf{u}|$ results in an alteration of the kinetic energy, the change of orientation results in the adjustment (shearing) of the wave number in accordance to the incompressibility equation ($\mathbf{k} \cdot \mathbf{u} = 0$).

Considering this chain of processes during a period of time, i.e., for some iterations, the proposed mechanical picture constructs a quantitative exact time behavior of all physical quantities. Here the direction of the perturbation velocity, and consequently the wave vector, continuously changes in time. This process is equivalent to a permanent clockwise rotation of the maximum pressure lines. Moreover, as the speed of sound in incompressible flows is infinite and the pressure instantly adjusts itself to any changes of the velocity field, the lines of constant pressure directly follow any change of the direction of the perturbation velocity. Hence, the line of maximum pressure is always parallel to the direction of the perturbation velocity.

At the moment the constant pressure lines of the Kelvin mode become parallel to the y axis ($k_y/k_x = 0$), the increase of energy is interrupted due to the zero collision angle with the wall and the angle between $\mathbf{u}$ and $\delta\mathbf{u}$ is $\theta = \pi/2$. With the continuing rotation ($k_y/k_x < 0$) the angle θ becomes obtuse and, hence, $|\mathbf{u} + \delta\mathbf{u}| < |\mathbf{u}|$. This is equivalent to a decrease of energy of the SFH, giving its energy back to the mean flow.

B. A quantitative analysis

In the following, the above presented qualitative analysis is validated by quantitative results stemming from simple physical reasonings and mathematical relations, which are based on Fig. 2. Herein, some iteration i is sketched and quantitatively described by adopting a simple constant time-stepping scheme with $t_{i+1} = t_i + \delta t_i$. At t_i the distance $\delta y(t_i)$ that the single fluid particle shifts along the y axis during a small period of time δt_i can be expressed as $\delta y(t_i) = u_y(t_i)\delta t_i$. This level deviation leads to the additional streamwise velocity of the fluid particle $\delta\mathbf{U}(t_i) = (-A\, u_y(t_i)\, \delta t_i, 0)$. This additional velocity is the collision velocity as it leads to the collision of the particle with the pressure wall (see Fig. 2). The collision transforms $\delta\mathbf{U}(t_i)$ into the additional perturbation velocity $\delta\mathbf{u}(t_i)$, which, in accordance to the elastic collision laws, is defined as

$$\begin{aligned} \delta u_x(t_i) &= -A u_y(t_i)\delta t_i \cos[\pi - 2\varphi(t_i)], \\ \delta u_y(t_i) &= A u_y(t_i)\delta t_i \sin[\pi - 2\varphi(t_i)], \end{aligned} \tag{2}$$

where $\varphi(t_i)$ is the angle between $\mathbf{k}$ and $\delta\mathbf{U}_i$ (i.e., the x axis). Thus, the perturbation velocity after the iteration has changed to

$$\mathbf{u}(t_{i+1}) = \mathbf{u}(t_i) + \delta\mathbf{u}(t_i). \tag{3}$$

Equation (3) gives the relation for the pre- and post-collision values of the perturbation velocities at $\delta t_i \to 0$,

$$\mathbf{u}_{i+1}^2 = \mathbf{u}_i^2 + \delta\mathbf{u}_i^2 + 2|\mathbf{u}_i||\delta\mathbf{u}_i| \cos\theta(t_i) \approx \mathbf{u}_i^2 + 2|\mathbf{u}_i||\delta\mathbf{u}_i| \cos\theta(t_i), \tag{4}$$

where $\theta(t_i)$ is the angle between $\delta\mathbf{u}_i$ and $\mathbf{u}_i$, with $\delta\mathbf{u}_i \ll \mathbf{u}_i$. According to Eq. (4) the value of the perturbation velocity increases ($\mathbf{u}_{i+1}^2 - \mathbf{u}_i^2 > 0$), just if $\cos\theta(t_i) > 0$, or equally $|\theta(t_i)| < \pi/2$. Combining Eqs. (2) and (4) and the trigonometric relation

$$\tan\varphi(t_i) = \frac{k_y(t_i)}{k_x}, \tag{5}$$

it is straightforward to derive

$$\cos\theta(t_i) = \frac{k_y(t_i)}{k(t_i)}, \tag{6}$$

which underlines that for $k_y(t_i) > 0$ the perturbation energy grows as $\theta(t_i) < \pi/2$ and vice versa.

Moreover, using Eq. (5), Eqs. (2) can be rewritten in terms of the time dependent wave number $\mathbf{k} = (k_x, k_y(t_i))$:

$$\frac{\delta u_x(t_i)}{\delta t_i} = Au_y(t_i)\frac{k_x^2 - k_y^2(t_i)}{k^2(t_i)}, \quad \frac{\delta u_y(t_i)}{\delta t_i} = 2Au_y(t_i)\frac{k_x k_y(t_i)}{k^2(t_i)}, \tag{7}$$

where $k^2(t_i) = k_x^2 + k_y^2(t_i)$. System (7) describes the variation of the perturbation velocity components during the iteration and tends towards the differential form for $\delta t_i \to 0$:

$$\frac{\partial u_x}{\partial t} = Au_y\frac{k_x^2 - k_y^2(t)}{k^2(t)}, \quad \frac{\partial u_y}{\partial t} = Au_y\frac{2k_x k_y(t)}{k^2(t)}, \tag{8}$$

which are the well-known 2D linearized Euler equations.

In fact, the variation of the momentum of the fluid particle in x direction at the ith iteration is defined by

$$m[\delta u_x(t_i) - \delta U_x(t_i)] = F_x\delta t_i, \tag{9}$$

where $m = \rho_0 V, \rho_0$, and V are the mass, density, and volume of the fluid particle, respectively. Further $\delta U_x(t_i) = -Au_y(t_i)\delta t_i$ and $F_x(t_i) = -ik_x p(t_i)V$, while δu_x is given by Eq. (2), so that the equation for the pressure is obtained for $\delta t_i \to 0$:

$$p(t) = iA\rho_0\frac{2k_x}{k^2(t)}u_y(t). \tag{10}$$

Finally, combining Eqs. (8) and (10) we get

$$\frac{\partial u_x}{\partial t} + Au_y = -ik_x\frac{p}{\rho_0}, \quad \frac{\partial u_y}{\partial t} = -ik_y(t)\frac{p}{\rho_0}, \tag{11}$$

which represents the full set of the linearized Euler equations (see the Appendix).

III. THE MECHANICAL PICTURE OF THE 3D TRANSIENT GROWTH

The mechanical picture of the transient growth in 3D with the base flow given by $\mathbf{U} = (Ay,0,0)$ is inherently identical to its 2D counterpart. Again, the countermotion of the neighboring sets of incompressible fluid particles compresses the medium and thereby forms a pressure perturbation field with maximums at the interfaces (planes) of the countermoving sets. Although the degrees of freedom of these interfaces, i.e., the maximum pressure planes (MPP) [defined by $k_x x + k_y(t)y + k_z z = 2\pi m$, with $m = 0, \pm1, \pm2, \ldots$], increase in the sense of rotation, the derivation of the full set of linearized Euler equations and the qualitative relations are insignificantly more difficult than in Sec. II B.

As for 2D perturbations, the dynamics of a single fluid particle inside the pressure field can be understood as a sequence of the same two processes: (1) deviation or, one can say shift of the fluid particle due to the shearwise perturbation velocity u_y from the level y to the level $y = (y - \delta y)$ and (2) elastic collision of the fluid particle with the MPP due to the additional streamwise perturbation

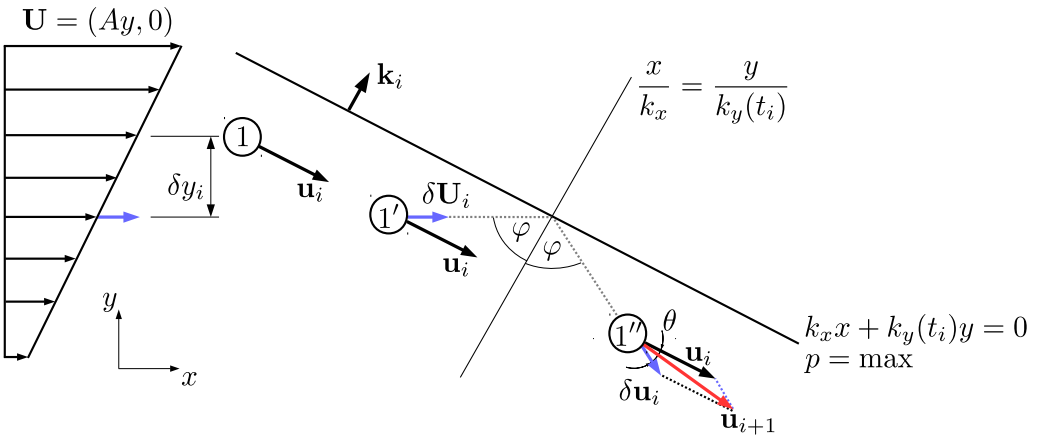

FIG. 3. Simplified sketch pointing out the mechanical feature of the reflection at the pressure wall ($p = \max$).

velocity (collision velocity), $\delta\mathbf{U}$. This mechanism is illustrated in Fig. 4, generalizing Fig. 3 for one particular ith iteration in three dimensions.

A. Extension of a quantitative analysis for 3D

Considering 3D perturbation dynamics, we exclusively operate in terms of line and plane equations. In this case the deviations by the collision entirely take place in a single plane; the elastic collision plane (ECP). For simplicity $m = 0$ is chosen in Fig. 4 and throughout the presented derivations. Hence, the equations for the MPP and ECP at the ith iteration can be written as

$$\text{MPP:} \quad k_x \cdot x + k_y(t_i) \cdot y + k_z \cdot z = 0, \quad \text{ECP:} \quad 0 \cdot x + k_z \cdot y - k_y(t) \cdot z = 0. \tag{12}$$

In the ECP the fluid particles undergo

(1) Collision (line $\overline{\text{AO}}$), with velocity $\delta\mathbf{U}(t_i) = (\delta U(t_i), 0, 0)$ and
(2) Reflection (line $\overline{\text{OB}}$), with velocity $\delta\mathbf{u}(t_i) = (\delta u_x(t_i), \delta u_y(t_i), \delta u_z(t_i))$.

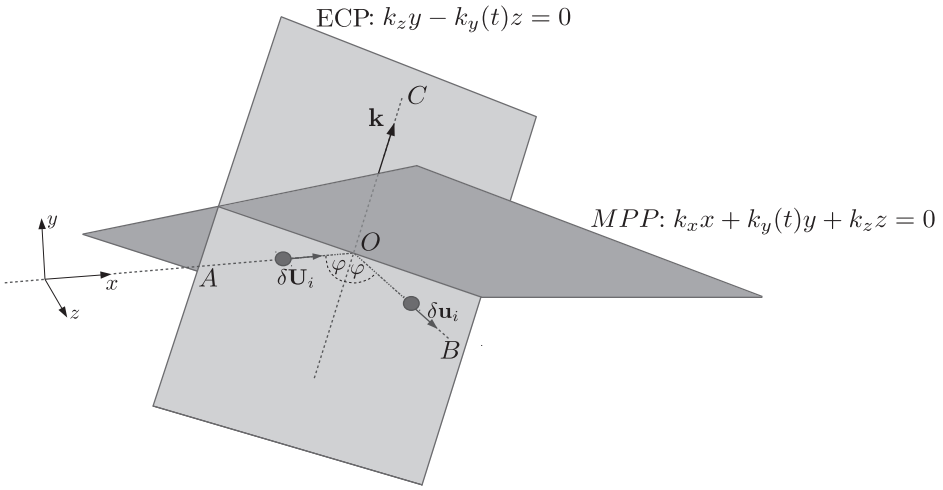

FIG. 4. Sketch of the elastic reflection of fluid particle from the "pressure wall."

Both lines, $\overline{\mathrm{AO}}$ and $\overline{\mathrm{OB}}$, as well as the line perpendicular to the MPP, $\overline{\mathrm{OC}}$, that has the same orientation as the wave number vector $\mathbf{k}(t_i) = (k_x, k_y(t_i), k_z)$, are located in the ECP. The equations of these lines can be summarized as

$$\overline{\mathrm{AO}}: \quad \frac{x}{\delta U(t_i)} = \frac{y}{0} = \frac{z}{0}, \quad \overline{\mathrm{BO}}: \quad \frac{x}{\delta u_x(t_i)} = \frac{y}{\delta u_y(t_i)} = \frac{z}{\delta u_z(t_i)}, \quad \overline{\mathrm{CO}}: \quad \frac{x}{k_x} = \frac{y}{k_y(t_i)} = \frac{z}{k_z}. \tag{13}$$

The angle included by $\overline{\mathrm{AO}}$ and $\overline{\mathrm{OC}}$ is the collision angle, while the one included by $\overline{\mathrm{OB}}$ and $\overline{\mathrm{OC}}$ the reflecting one. Due to the elastic collision, these angles, denoted by $\varphi(t_i)$, as well as the absolute values of the collision and reflection velocities are equal, thus, $|\delta\mathbf{U}(t_i)| = \sqrt{|\delta\mathbf{u}(t_i)|^2}$.

The equation for the ECP (12) can be rewritten in terms of the postcollision perturbation deviations $\delta\mathbf{u}(t_i)$ by recognizing that the lines $\overline{\mathrm{AO}}$ and $\overline{\mathrm{OB}}$ are located in this plane:

$$\mathrm{ECP}: \quad \frac{y}{\delta u_y(t_i)} - \frac{z}{\delta u_z(t_i)} = 0. \tag{14}$$

Using Eqs. (12) and (14) it can be shown that $k_y(t_i)/k_z = \delta u_z(t_i)/\delta u_y(t_i)$. As a result, $\varphi(t_i)$ is defined only by the wave numbers:

$$\cos\varphi(t_i) = \frac{k_x}{k(t_i)}, \quad \text{with } k^2(t_i) = k_x^2 + k_y^2(t_i) + k_z^2. \tag{15}$$

Up to this point, the derivation of the fluid particle streamwise velocity perturbation equation is almost identical to the one proposed in two dimensions. Following the procedure (2)–(8) we derive

$$\delta u_x(t_i) = -Au_y(t_i)\delta t_i \cos[\pi - 2\varphi(t_i)] = Au_y(t_i)\delta t_i \frac{k_x^2 - k_y^2(t_i) - k_z^2}{k^2(t_i)}, \tag{16}$$

with $\cos 2\varphi(t_i) = \delta u_x(t_i)/\delta U$. Combining Eqs. (12) and (14) together with $|\delta\mathbf{U}(t_i)| = \sqrt{|\delta\mathbf{u}(t_i)|^2}$ the deviations of the shearwise and spanwise velocity perturbations of a single fluid particle at the ith iteration are derived:

$$\delta u_y(t_i) = 2Au_y(t_i)\delta t_i \frac{k_x k_y(t_i)}{k^2(t_i)}, \tag{17}$$

$$\delta u_z(t_i) = 2Au_y(t_i)\delta t_i \frac{k_x k_z}{k^2(t_i)}. \tag{18}$$

For the limit $\delta t_i \to 0, \delta u_x(t_i)/\delta t_i = \partial u_x/\partial t$ and Eqs. (16)–(18) become

$$\frac{\partial u_x(t)}{\partial t} = Au_y \frac{k_x^2 - k_y^2(t) - k_z^2}{k^2(t_i)}, \quad \frac{\partial u_y(t)}{\partial t} = 2Au_y \frac{k_x k_y(t)}{k^2(t_i)}, \quad \frac{\partial u_z(t)}{\partial t} = 2Au_y \frac{k_x k_z}{k^2(t_i)}. \tag{19}$$

Consequently, the linearized Euler equations (A8)–(A10) have been reconstructed for three dimensions from the proposed physics. Hereby, the particle collision with the MPP has been considered only on one side, while the same process takes place on the other side of the plane, equivalent to particles 1 and 2 in Fig. 2(b), for a multitude of virtual fluid particles.

B. The dependence of the transient energy growth on the collision angle

We analyze the temporal evolution of the (kinetic) perturbation energy, defined as $E_{\mathbf{k}}(t) = |\mathbf{u}(t)|^2$ for a single plane wave, in the framework of the proposed mechanical picture. As for the 2D case, at the ith iteration (equals to $\mathbf{u}_{i+1}^2 - \mathbf{u}_i^2$) the variation of the energy is defined by Eq. (4). As a consequence, there exists a direct connection between $\theta(t_i)$ and the energy variation of the wave; the energy growth or decay is determined solely by this angle. Using Eqs. (16)–(18) and (A8)–(A10) one can express $\cos\theta(t_i)$ via $k_x, k_y(t_i), k_z, u_y(0)$ and C [similar to the 2D case; see Eq. (6)]. Although the derivation is straightforward, the final expression of $\cos\theta(t_i)$ is lengthy, so it is not presented

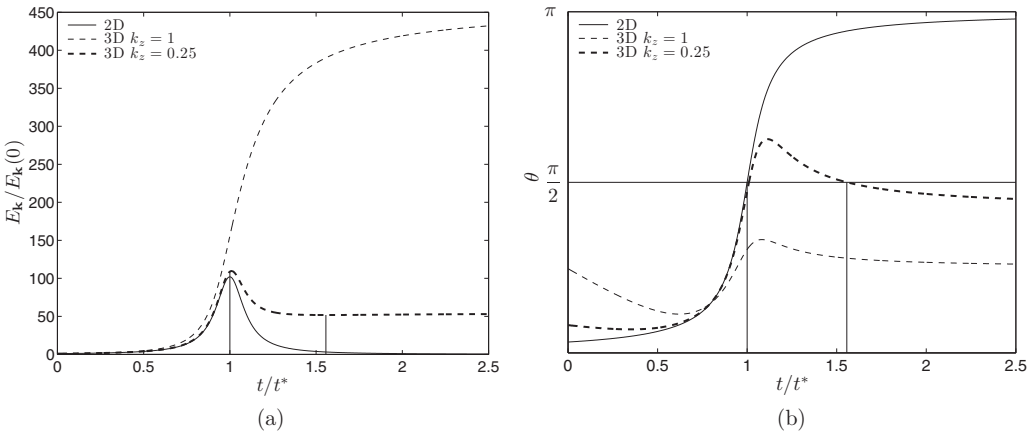

FIG. 5. Evolution of (a) the 2D and 3D Kelvin mode normalized energy $E_{\mathbf{k}}(t)/E_{\mathbf{k}}(0)$ and (b) the angle $\theta(t) = \measuredangle(\mathbf{u}, \delta\mathbf{u})$ for the following sets of parameters: $A = 0.05, k_x = 1, k_y(0) = 10$, and $k_z = 0$ (solid lines), $k_z = 1$ (thin dashed lines), $k_z = 0.25$ (thick dashed lines); $C/u_y(0) = 0.1$ for the latter two.

here. We rather present plots of the evolution of (a) $E_{\mathbf{k}}(t)$ and (b) $\theta(t)$ for three sets of parameters in Fig. 5 and compare their time evolutions.

The solid lines show that, for the 2D wave, $\theta(t)$ becomes obtuse at times $t = t^* = k_y/Ak_x$ and, consequently, from this moment on the growth of $E_{\mathbf{k}}(t)$ is changed by its attenuation. The thin dashed lines show that the energy of the 3D wave with $k_x = k_z = 1$ and $C/u_y(0) = 0.1$ monotonically increases, as $\theta(t)$ is always acute. Yet the situation changes for a wave with small $k_z = 0.25$ (thick dashed lines): for the time interval $1 \lesssim t/t^* \lesssim 1.6$ the angle $\theta(t) > \pi/2$, and, as it was expected, the energy decays. Outside of this time interval, where the angle is acute, the energy increases. Summarizing, the energy growth of the Kelvin modes is exclusively defined by the angle θ and that the maximal growth is observed at minimal θ. In fact, the perturbation energy grows only if $\theta(t) < \pi/2$, while it is given back to the mean flow for angles of $\theta(t) > \pi/2$.

IV. DISCUSSION AND CONCLUSIONS

A mechanical picture of the linear transient energy growth is presented on the basis of the dynamics of the simplest form of perturbations (referred to as Kelvin mode, plane wave, or spatial Fourier harmonics of perturbations) in an inviscid unbounded plane constant shear flow. Besides the simplicity, the advantage of the regarded plane perturbations is the fact that they form the complete basis and any perturbation can be presented as a sum or integral of Kelvin modes.

A. Summary of the proposed mechanical picture

The proposed mechanical picture quantitatively exactly describes the transient growth process including the cause and moment of alteration of the growth by attenuation. As it is equally applicable for 2D and 3D perturbations, the universal nature of the transient growth physics is suggested. However, the most important result is the fact that the presented mechanical picture allows us to reconstruct the linearized Euler equations. This points to the basic nature and exactness of the presented mechanism that easily and naturally explains the nuances of the transient growth, i.e., the 3D maximal growth rates are by an order of magnitude larger than the corresponding 2D ones and are attained at later stages, namely, when the Kelvin modes are tilted with the background shear.

These modes form an alternation of countermoving layers with a periodic velocity field, which interact with the basic shear velocity field. This interplay leads to a pressure perturbation field with extrema at the border planes of the countermoving layers. We emphasize that the pressure force is

the key player of the energy exchange processes, the main factor of the dynamical activity. Hence, it should not be disregarded when analyzing the energy exchange processes, despite the fact that this force does not contribute to the overall energy budget. This, on the one hand, is in accordance with the role of the pressure in isotropic turbulence, where the pressure forces have a nonlinear origin and are responsible for the redistribution of kinetic energy among fluid elements, also without making a net contribution to the overall energy budget. It is characteristic that the physical mechanisms of this redistribution are fundamentally different in 2D and 3D cases (see discussion in Sec. I). In this context one should note that by considering the linear transient perturbation dynamics any nonlinear effects are excluded, and the linear pressure terms reveal their universal nature in two and three dimensions, in contrast to the nonlinearly originated pressure terms.

To comprehend the role of the pressure forces in the investigated dynamical processes, we find it helpful to present an analogy from the field of chemistry: A particular class of chemical reactions takes place only at the presence of a catalyst. Schematically, the role of the pressure force, namely, the role of the elastic collision of fluid particles with constant pressure planes, is similar to the role of the catalyst in this class of chemical reactions. Although the catalyst is not involved in any balances, the chemical reaction will not proceed without it, and, thus, the analysis of the role of the catalyst is essential for the basic understanding of this class of reactions.

To construct the mechanical picture of the transient dynamics, we replaced the continuous fluid dynamics by one of the multiple virtual fluid particles, as sketched in Fig. 2(a) and subsequently analyzed the countermotion of neighboring sets (white and gray zones) of the fluid particles in the shear flow. Our presentation is thereby based on the description of three processes in the following order: (1) the interplay of two single, distinct (virtual) fluid particles with the background flow; (2) generalization on a large amount of such particles, interacting with each other and thereby inducing a pressure wall; and (3) the description of the interaction of the multitude of fluid particles with the formed pressure perturbation wall.

As described in Sec. II B, the multitude of the fluid particles from the white zone are shifted downwards (as for them $u_y < 0$) and, in their new location, move faster in the streamwise direction compared to the background flow. This increases the streamwise velocity of the fluid particles from the white zone, leading to the appearance of an additional streamwise velocity directed from left to right. The same applies for a multitude of fluid particles from the gray zone, but in the opposite direction. These counterdirected velocities that originate from the white and gray zones and that have been labeled as collision velocities lead to a compression. For this compression an increase of the collision velocity is necessary, which occurs due to the increase of $|u_y|$. The latter happens at $k_y(t)/k_x > 0$, i.e., in the case presented in Fig. 2. At $k_y(t)/k_x < 0$, the shifting of the countermoving fluid particles reduces, as does $|u_y|$, initiating the reduction of the collision velocity and, consequently, the decompression. So at $k_y(t)/k_x > 0$ the countermoving neighboring sets of fluid particles (white and gray zones) are compressed at the lines of $k_x x + k_y y = 2\pi m$, leading to the creation of a pressure field. This pressure field increases in the vicinity of this line and achieves its maximum value at $k_y(t) = 0$. The related decompression phase of the countermoving neighboring sets occurs afterwards at $k_y(t)/k_x < 0$, and the pressure perturbation reduces again. The formulated pressure dynamics matches the one described by Eq. (10).

This pressure field (created by the countermoving fluid particles), in its turn, acts back on the fluid particles as follows: The pressure field may be considered as a "pressure wall," and the motion of any fluid particle can be considered in terms of collisions with this pressure wall. Due to the appearance of the collision velocity, each fluid particle undergoes an elastic collision with the pressure wall, leading to a change of the collision velocity in accordance to the classical theory of elastic collision of particles with a rigid wall. Thereby the absolute value as well as the direction of the fluid particles velocities continuously change, which then equal the (continuous) fluid perturbation velocity. While the change in the absolute values of the velocity results in a change of the kinetic energy of the regarded Kelvin mode, the change in direction results in the shearing of the respective wave number ($\mathbf{k} \cdot \mathbf{u} = 0$). As the compression phase is followed by the decompression one, we conclude that it is a precursor of the transient nature of the dynamics.

B. Further discussion

The physical explanation in terms of the mechanical picture benefits from its ease, and, although it is constructed for vortex mode perturbations, it can be naturally generalized for the energy transient growth of wave perturbations in different, e.g., compressible, stratified, magnetized, shear flows. Specifically the linear spontaneous generation of waves by vortex disturbances is rather widespread and well described in compressible [24–28], stratified [29–32], and magnetized [33,34] shear flows. The generation is the result of the linear coupling of vortex and wave modes, which mathematical ground is the shear flow nonnormality. Consequently, it differs from that considered in Lighthill's seminal papers [35,36] and, generally, from different formulations of the acoustic analogy (AA). By comparing the topologies of the nonnormality induced mechanism of linear wave generation and of the "source" terms of the classical AA formulations, Hau *et al.* [28] have shown the incompatibility between them; any of these "sources" miss the described anisotropy of linear sound generation in shear flows and therefore indicate an issue of the linear part of the source term description in AAs. The linear vortex-wave coupling is in fact asymmetric: A vortex mode, having nonzero potential vorticity, is able to generate a wave mode, having zero potential vorticity, but not vice versa.

One has to note, that the process of wave generation proceeds analogically and is described by similar mathematics for all kinds of shear flows; at small shear rates, the wave generation is exponentially small and is described by the techniques of exponential asymptotics and the occurrence of a Stokes phenomenon, while at moderate and large shear rates, the wave generation is described just numerically. Despite the success of mathematical description of the linear dynamics for both small and large shear rates, the generic root (physical essence) of the linear wave generation by vortex disturbances has not been described so far, because the specific physics are different for different (e.g., compressible, stratified, and magnetized) shear flows. However, the wave generation by vortex mode harmonics due to the change in the pressure compression phase by decompression at the moment $t = t^*$ [i.e., when $k_y(t^*) = 0$] is found to be the common feature between these phenomena. The description of these wave generation process based on the proposed mechanical picture is the subject of future work.

ACKNOWLEDGMENT

G. Chagelishvili would like to acknowledge the hospitality of TU Darmstadt and DFG Project GZ:OB 96/38-1 AOBJ: 578003.

APPENDIX: LINEARIZED EULER EQUATIONS FOR THE KELVIN MODES IN INVISCID PLANE CONSTANT SHEAR FLOWS

The linearized Euler equations for perturbed variables in incompressible, unstratified, plane parallel shear flow, $\mathbf{U}_0 = (Ay,0,0)$, have the form

$$\left(\frac{\partial}{\partial t} + Ay\frac{\partial}{\partial x}\right)u_x + Au_y = -\frac{1}{\rho_0}\frac{\partial p}{\partial x}, \tag{A1}$$

$$\left(\frac{\partial}{\partial t} + Ay\frac{\partial}{\partial x}\right)u_y = -\frac{1}{\rho_0}\frac{\partial p}{\partial y}, \tag{A2}$$

$$\left(\frac{\partial}{\partial t} + Ay\frac{\partial}{\partial x}\right)u_z = -\frac{1}{\rho_0}\frac{\partial p}{\partial z}, \tag{A3}$$

where ρ_0 is the density, (u_x,u_y,u_z) and p are velocity and pressure perturbations, correspondingly. The continuity equation in this case has the form

$$\frac{\partial u_x}{\partial x} + \frac{\partial u_y}{\partial y} + \frac{\partial u_z}{\partial z} = 0. \tag{A4}$$

Equations (A1)–(A4) permit the decomposition of perturbed variables into Kelvin modes (or the same as plane wave; spatial Fourier harmonics) with time-dependent amplitudes and phases

$$\Phi(\mathbf{x},t) = \Phi(\mathbf{k}(t),t)\cdot\exp[ik_x x + ik_y(t)y + ik_z z], \quad k_y(t) = k_y(0) - Ak_x t, \tag{A5}$$

where $\Phi \equiv (u_x, u_y, u_z, p)$. It should also be noted that the Kelvin mode represents the basic "element" of dynamical processes at constant shear rate [37] and greatly helps to understand transient phenomena in shear flows.

Substituting Eq. (A5) into Eqs. (A1)–(A4), we get the following system of first order ordinary differential equations that govern the linear dynamics of Kelvin modes:

$$\frac{\partial u_x}{\partial t} + Au_y = -ik_x\frac{p}{\rho_0}, \quad \frac{\partial u_y}{\partial t} = -ik_y(t)\frac{p}{\rho_0},$$
$$\frac{\partial u_z}{\partial t} = -ik_z\frac{p}{\rho_0}, \quad k_x x + k_y(t)y + k_z z = 0. \tag{A6}$$

This system allows one to find the following algebraic expression for the pressure perturbation

$$p = iA\rho_0\frac{2k_x}{k^2(t)}u_y, \tag{A7}$$

and, finally, eliminating the pressure term from the system, one gets

$$\frac{\partial u_x}{\partial t} = A\left[\frac{2k_x^2}{k^2(t)} - 1\right]u_y, \tag{A8}$$
$$\frac{\partial u_y}{\partial t} = A\frac{2k_x k_y(t)}{k^2(t)}u_y, \tag{A9}$$
$$\frac{\partial u_z}{\partial t} = A\frac{2k_x k_z}{k^2(t)}u_y, \tag{A10}$$

where $k^2(t) \equiv k_x^2 + k_y^2(t) + k_z^2$.

For the considered problem there exists the well-known complete set of analytic solutions (see Refs. [38–40]):

$$u_x(t) = -\frac{k_z C}{k_x} - u_y(0)\frac{k^2(0)k_x k_y(t)}{k^2(t)\left(k_x^2+k_z^2\right)}$$
$$+ u_y(0)\frac{k^2(0)k_z^2}{k_x\left(k_x^2+k_z^2\right)^{\frac{3}{2}}}\left[\arctan\frac{k_y(t)}{\left(k_x^2+k_z^2\right)^{\frac{1}{2}}} - \arctan\frac{k_y(0)}{\left(k_x^2+k_z^2\right)^{\frac{1}{2}}}\right], \tag{A11}$$
$$u_y(t) = \frac{k^2(0)}{k^2(t)}u_y(0), \tag{A12}$$
$$u_z(t) = C - u_y(0)\frac{k^2(0)k_z k_y(t)}{k^2(t)\left(k_x^2+k_z^2\right)}$$
$$- u_y(0)\frac{k^2(0)k_z}{\left(k_x^2+k_z^2\right)^{\frac{3}{2}}}\left[\arctan\frac{k_y(t)}{\left(k_x^2+k_z^2\right)^{\frac{1}{2}}} - \arctan\frac{k_y(0)}{\left(k_x^2+k_z^2\right)^{\frac{1}{2}}}\right], \tag{A13}$$

where $u_y(0)$ is the shearwise velocity of the initial Kelvin mode (plane wave), C, a free parameter that, together with $u_y(0)$, defines the rest components of the initial Kelvin mode:

$$u_x(0) = -\frac{k_z C}{k_x} - u_y(0)\frac{k_x k_y(0)}{\left(k_x^2+k_z^2\right)}, \quad u_z(0) = C - u_y(0)\frac{k_z k_y(0)}{\left(k_x^2+k_z^2\right)}. \tag{A14}$$

Equation (A6) or, in the reduced form, Eqs. (A8)–(A10) represent the linearized Euler equations for a single Kelvin mode in the considered flow. In two dimensions, $k_z = 0$, the equations reduce to

$$\frac{\partial u_x}{\partial t} = A\frac{k_x^2 - k_y^2(t)}{k_x^2 + k_y^2(t)}u_y, \quad \frac{\partial u_y}{\partial t} = A\frac{2k_x k_y(t)}{k_x^2 + k_y^2(t)}u_y. \tag{A15}$$

[1] L. H. Gustavsson, Energy growth of three-dimensional disturbances in plane Poiseuille flow, J. Fluid Mech. **224**, 241 (1991).

[2] D. S. Henningson, L. H. Gustavsson, and K. S. Breuer, Localized disturbances in parallel shear flows, Appl. Sci. Res. **53**, 51 (1994).

[3] P. J. Schmid and D. S. Henningson, *Stability and Transition in Shear Flows*, Applied Mathematical Sciences Vol. 142 (Springer, New York, 2001).

[4] T. Betcke and L. N. Trefethen, Reviving the method of particular solutions, SIAM Rev. **47**, 469 (2005).

[5] P. J. Schmid, Nonmodal stability theory, Annu. Rev. Fluid Mech. **39**, 129 (2007).

[6] K. M. Butler and B. F. Farrell, Three-dimensional optimal perturbations in viscous shear flow, Phys. Fluids A **4**, 1637 (1992).

[7] B. F. Farrell and P. J. Ioannou, Generalized stability theory part. I. Autonomous operators, J. Atmos. Sci. **53**, 2025 (1996).

[8] L. Kelvin, Stability of fluid motion: Rectilinear motion of viscous fluid between two parallel plates, Philos. Mag. **24**, 188 (1887).

[9] G. D. Chagelishvili, R. G. Chanishvili, and D. G. Lominadze, Physics of the amplification of vortex disturbances in shear flows, JETP Lett. **63**, 543 (1996).

[10] A. Salhi and C. Cambon, Stability of rotating stratified shear flow: An analytical study, Phys. Rev. E **81**, 026302 (2010).

[11] R. S. Lindzen, Instability of plane parallel shear flow (toward a mechanistic picture of how it works), Pure Appl. Geophys. **126**, 103 (1988).

[12] E. N. Parker, The dynamical state of the interstellar gas and field, Astrophys. J. **145**, 811 (1966).

[13] S. A. Balbus and J. F. Hawley, A powerful local shear instability in weakly magnetized disks. IV. Nonaxisymmetric perturbations, Astrophys. J. **400**, 610 (1992).

[14] W. M. F. Orr, The stability or instability of the steady motions of a perfect liquid and of a viscous liquid. Part I: A perfect liquid, Proc. Roy. Irish Acad. Sect. A **27**, 9 (1907).

[15] M. T. Landahl, A note on an algebraic instability of inviscid parallel shear flows, J. Fluid Mech. **98**, 243 (1980).

[16] G. K. Batchelor, Pressure fluctuations in isotropic turbulence, Proc. Cambridge Philos. Soc. **47**, 359 (1951).

[17] R. J. Hill and S. T. Thoroddsen, Experimental evaluation of acceleration correlations for locally isotropic turbulence, Phys. Rev. E **55**, 1600 (1997).

[18] A. La Porta, G. A. Voth, A. M. Crawford, J. Alexander, and E. Bodenschatz, Fluid particle accelerations in fully developed turbulence, Nature (London) **409**, 1017 (2001).

[19] P. Vedula and P. K. Yeung, Similarity scaling of acceleration and pressure statistics in numerical simulations of isotropic turbulence, Phys. Fluids **11**, 1208 (1999).

[20] T. Gotoh and D. Fukayama, Pressure Spectrum in Homogeneous Turbulence, Phys. Rev. Lett. **86**, 3775 (2001).

[21] T. Gotoh and T. Nakano, Role of pressure in turbulence, J. Stat. Phys. **113**, 855 (2003).

[22] A. Pumir, H. Xu, G. Boffetta, G. Falkovich, and E. Bodenschatz, Redistribution of Kinetic Energy in Turbulent Flows, Phys. Rev. X **4**, 041006 (2014).

[23] G. Mamatsashvili, S. Dong, G. Khujadze, G. Chagelishvili, J. Jimenez, and H. Foysi, Homogeneous shear turbulence: bypass concept via interplay of linear transient growth and nonlinear transverse cascade, J. Phys. Conf. Ser. **708**, 012001 (2016).

[24] G. D. Chagelishvili, A. G. Tevzadze, G. Bodo, and S. S. Moiseev, Linear Mechanism of Wave Emergence from Vortices in Smooth Shear Flows, Phys. Rev. Lett. **79**, 3178 (1997).
[25] B. F. Farrell and P. J. Ioannou, Transient and asymptotic growth of two-dimensional perturbations in viscous compressible shear flow, Phys. Fluids **12**, 3021 (2000).
[26] N. A. Bakas, Mechanism underlying transient growth of planar perturbations in unbounded compressible shear flow, J. Fluid Mech. **639**, 479 (2009).
[27] G. Favraud and V. Pagneux, Superadiabatic evolution of acoustic and vorticity perturbations in Couette flow, Phys. Rev. E **89**, 033012 (2014).
[28] J.-N. Hau, G. Chagelishvili, G. Khujadze, M. Oberlack, and A. Tevzadze, A comparative numerical analysis of linear and nonlinear aerodynamic sound generation by vortex disturbances in homentropic constant shear flows, Phys. Fluids **27**, 126101 (2015).
[29] M. E. McIntyre, Spontaneous imbalance and hybrid vortex–gravity structures, J. Atmos. Sci. **66**, 1315 (2009).
[30] M. E. McIntyre, Potential vorticity, Encyc. Atmos. Sci. **2**, 685 (2003).
[31] A. G. Tevzadze, G. D. Chagelishvili, and J.-P. Zahn, Hydrodynamic stability and mode coupling in Keplerian flows: Local strato-rotational analysis, Astron. Astrophys. **478**, 9 (2008).
[32] J. Vanneste and I. Yavneh, Exponentially small inertia-gravity waves and the breakdown of quasi-geostrophic balance, J. Atmos. Sci. **61**, 211 (2004).
[33] A. G. Tevzadze, Velocity shear induced phenomena in solar and astrophysical flows, Ph.D. thesis, Katholieke Universiteit Leuven, 2006.
[34] T. Heinemann and J. C. B. Papaloizou, The excitation of spiral density waves through turbulent fluctuations in accretion discs. II. Numerical simulations with MRI-driven turbulence, Mon. Not. R. Astron. Soc. **397**, 64 (2009).
[35] M. J. Lighthill, On sound generated aerodynamically. I. General theory, Proc. R. Soc. London A **211**, 564 (1952).
[36] M. J. Lighthill, On sound generated aerodynamically. II. Turbulence as a source of sound, Proc. R. Soc. London A **222**, 1 (1954).
[37] Z. Yoshida, Kinetic theory for non-Hermitian dynamics of waves in shear flow, Phys. Plasmas **12**, 024503 (2005).
[38] H. K. Moffat, Interaction of turbulence with strong wind shear, in *Atmosphere Turbulence and Radio Wave Propagation*, edited by A. M. Yaglom and V. I. Tatarskii (Nauka Press, Moscow, 1967), p. 139.
[39] A. D. D. Craik and W. O. Criminale, Evolution of wavelike disturbances in shear flows: A class of exact solutions of the Navier-Stokes equations, Proc. R. Soc. London A **406**, 13 (1986).
[40] B. F. Farrell and P. J. Ioannou, Optimal excitation of three-dimensional perturbations in viscous constant shear flow, Phys. Fluids A **5**, 1390 (1993).